Supporting Information

of

Cucurbit[8]uril Regulated Activatable Supramolecular Photosensitizer for Targeted Cancer Imaging and Photodynamic Therapy†

Xiaoqiang Wang, Qi Lei, Jingyi Zhu, Wenjing Wang, Qian Cheng, Fan Gao, Yunxia Sun,* and Xianzheng Zhang*

Key Laboratory of Biomedical Polymers of Ministry of Education, the Institute for Advanced Studies & Department of Chemistry, Wuhan University, Wuhan 430072, P. R. China

* Corresponding Authors. yx-sun@whu.edu.cn (Y. X. Sun), xz-zhang@whu.edu.cn (X. Z. Zhang).

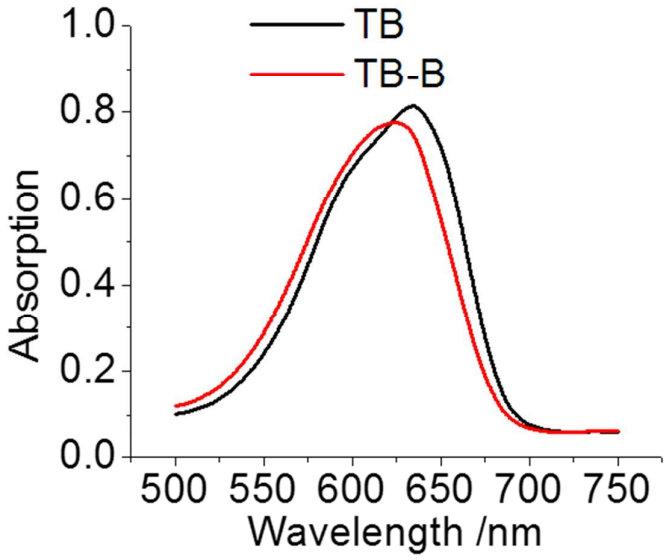

Figure S1. UV-VIS absorption of TB (20 μM) and TB-B (20 μM).

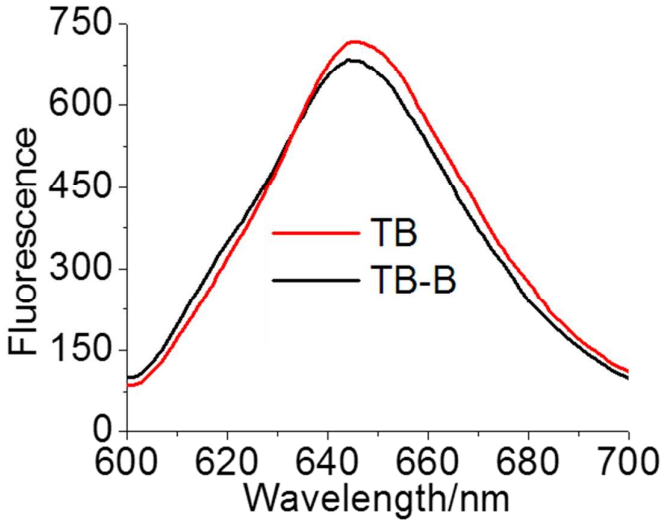

Figure S2. Fluorescence emission of TB (20 μM) and TB-B (20 μM).

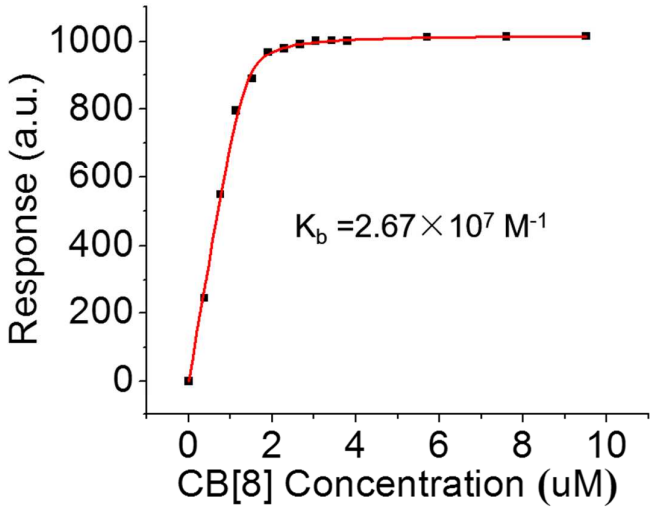

Figure S3. The binding curve of CB[8] and TB-B upon the titration of CB[8] (0-10 μM) into solution of TB-B (4 μM) in PBS (10mM, pH=7.4). Y-axis represent for the difference of TB-B fluorescence intensity at 647nm before and after the titration of CB[8].

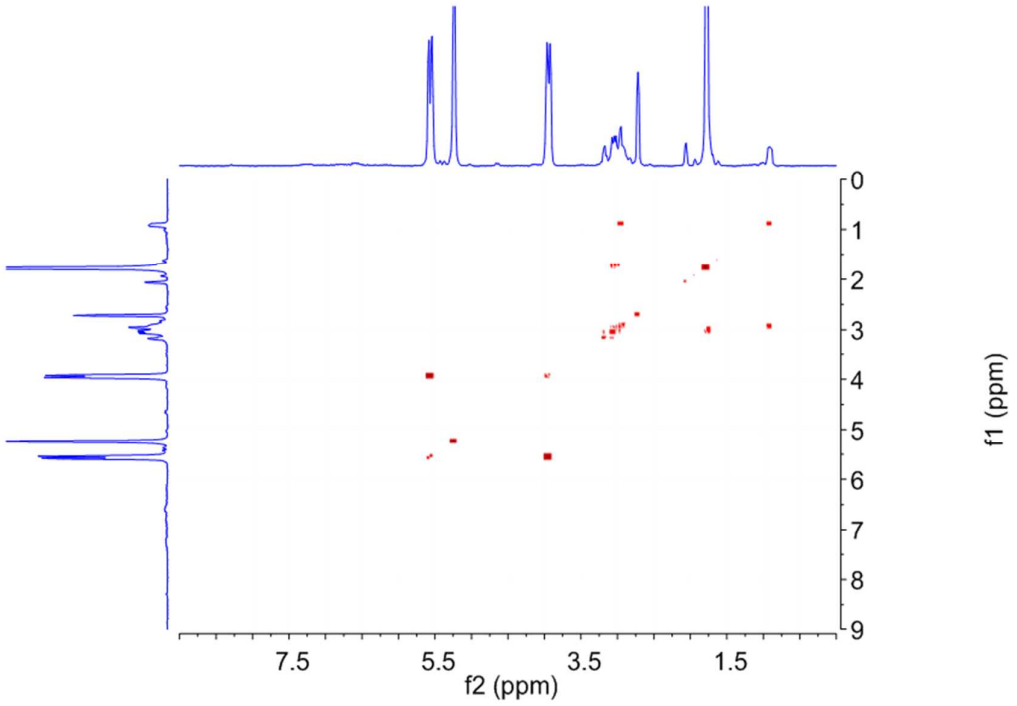

Figure S4. COSY NMR spectra of TB-B:CB[8] 2:1 (D_2O, 3 mM)

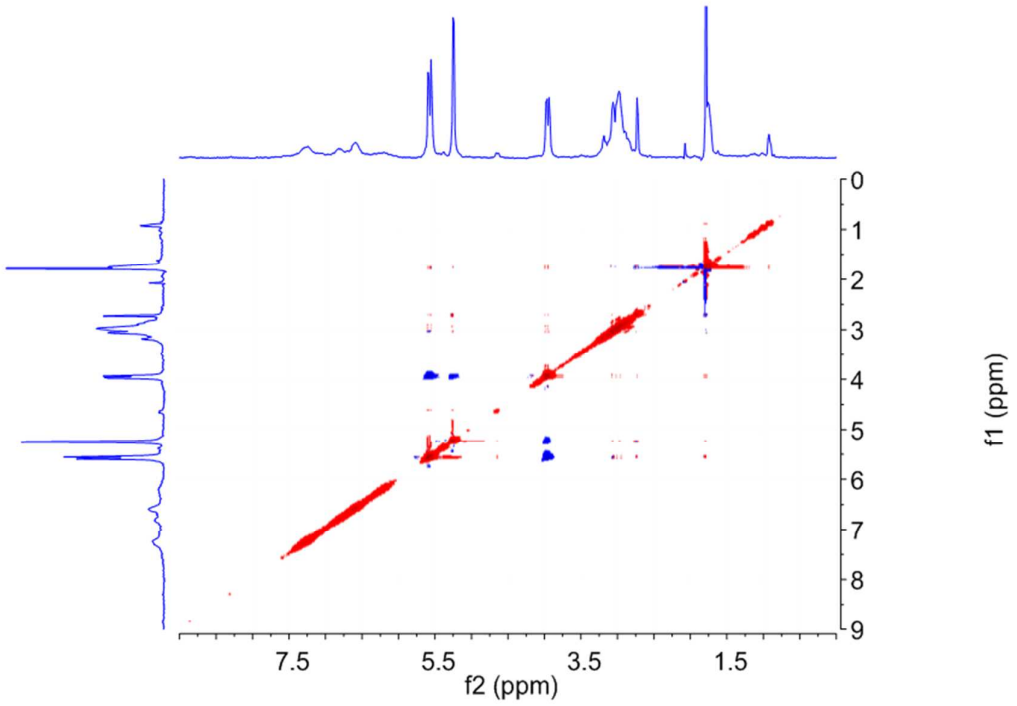

Figure S5. ROESY NMR spectra of TB-B:CB[8] 2:1 (D_2O, 3 mM).

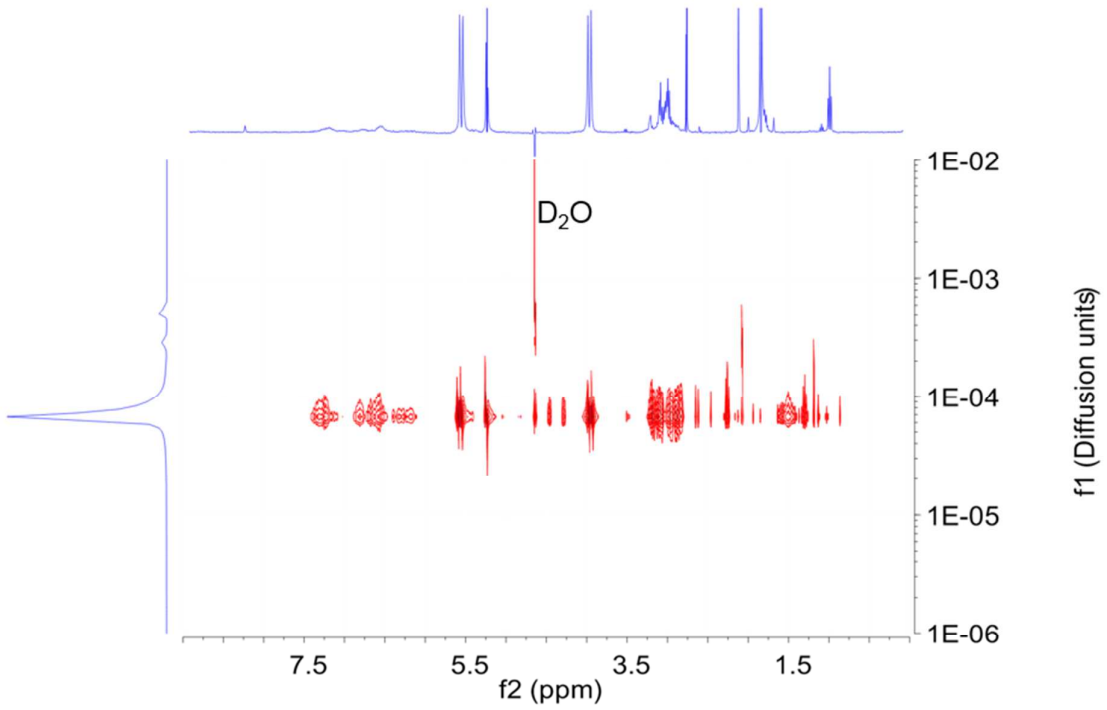

Figure S6. DOSY NMR spectra of TB-B:CB[8] 2:1 (D_2O, 3 mM).

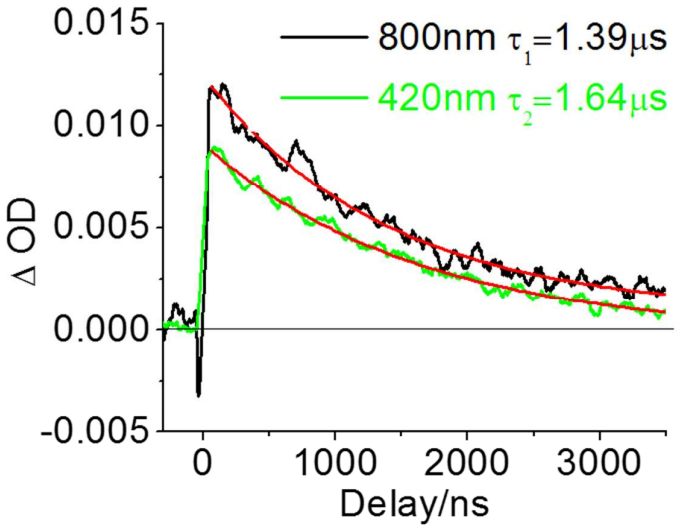

Figure S7. Decay curves of the transient absorption of TB-B at 420 nm and 800 nm.

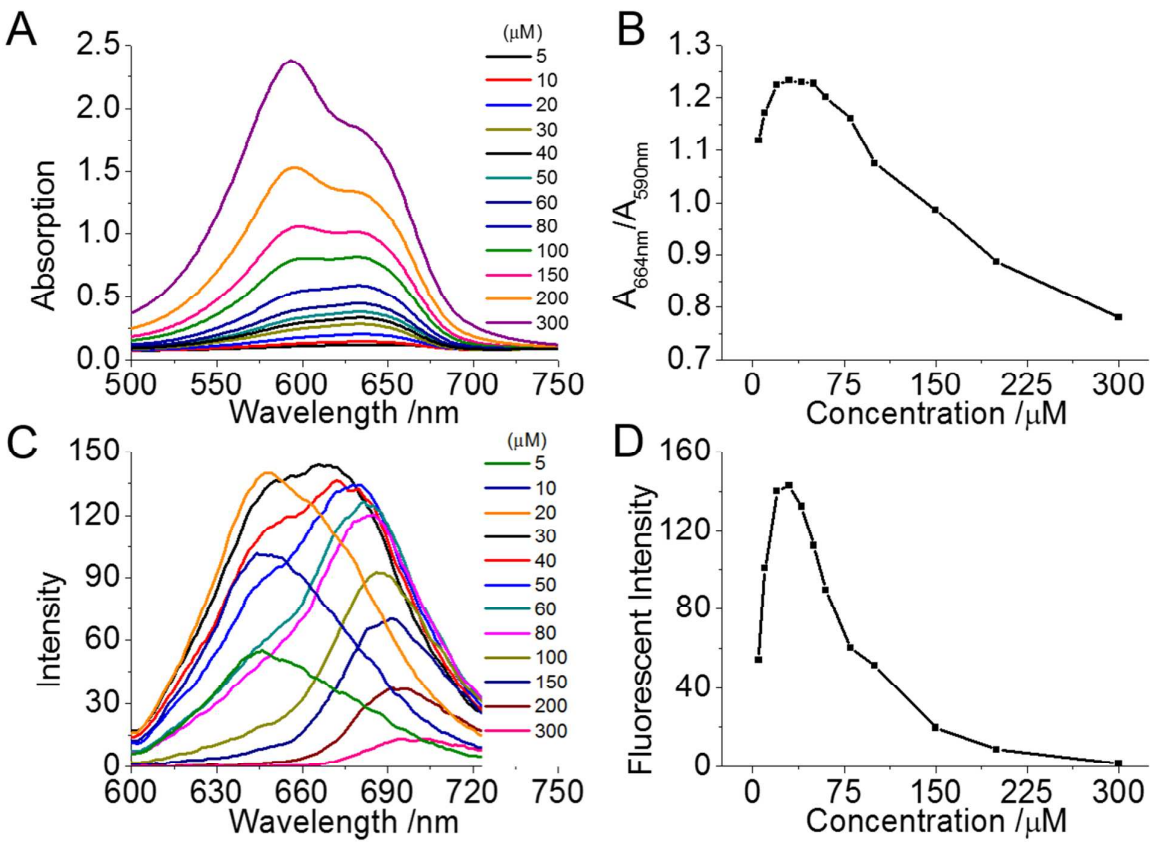

Figure S8. Optical properties of TB in different concentration. A) UV-Vis absorption of TB (5-300 μM) in PBS (10Mm, PH=7.4); B) Ratio of TB absorption at 630 nm (TB monomer absorption peak) and 590 nm (TB dimer absorption peak) in different concentration (5-300 μM); C) Fluorescent changes of TB (5-300 μM) in PBS (10Mm, PH=7.4); D) Fluorescent emmission of TB at 647 nm in different concentration (5-300 μM).

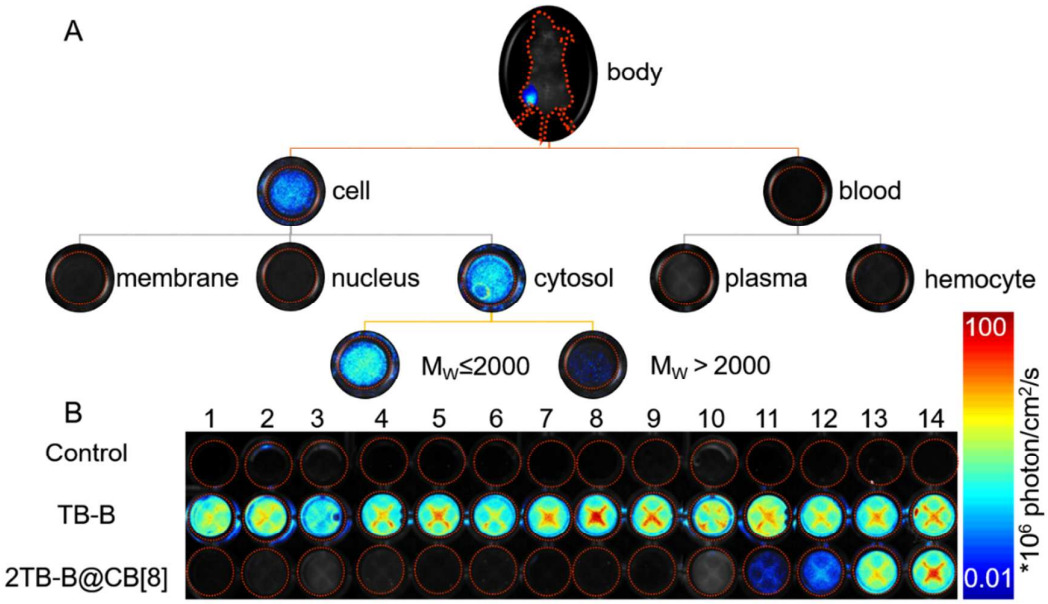

Figure S9. A) Separation of the components from the body and their influence to the fluorescence of 2TB-B@CB[8] imaged by *in vivo* imaging system;B)Fluorescent recovery of 2TB-B@CB[8] in various small molecular species (100μM in PBS). 1, glucose; 2, pyruvic acid; 3, glutamine; 4, lactic acid; 5, collection of salts (Na^+, K^+, Ca^{2+}, Mg^{2+}, Fe^{3+}, Zn^{2+}); 6, collection of 20 proteinogenic amino acids; 7, dipeptide GW; 8, dipeptide GY; 9, dipeptide GF; 10, dipeptide GG; 11, dipeptide WG; 12, dipeptide YG; 13, dipeptide FG; 14, tripeptide FGG.

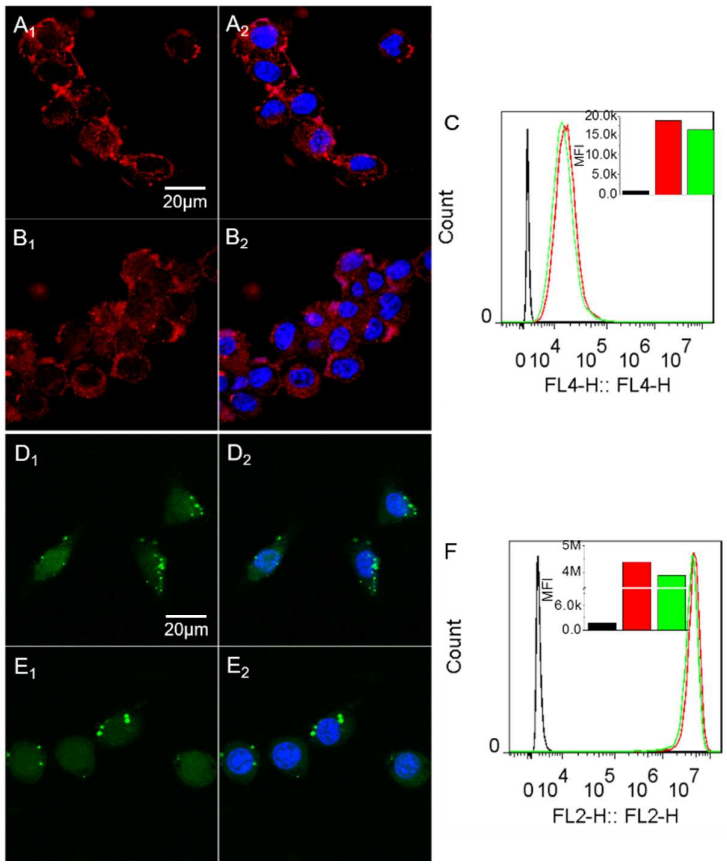

Figure S10. A-B) Confocal microscopy images showing SCC-7 cells incubated with A) TB-B (10 μM) and B) 2TB-B@CB[8] (5 μM) (red=TB, blue=nucleus); C) Quantitative flow cytometry analysis of the fluorescence of TB after SCC-7 cells incubated with TB-B (10 μM) and 2TB-B@CB[8] (5 μM) (black line=control, red line=TB-B, green line=2TB-B@CB[8], inset: mean fluorescence intensity (MFI) of TB); D-E) Confocal microscopy images showing intracellular ROS generation ability of D) TB-B (10 μM) and E) 2TB-B@CB[8] (5 μM) after incubated with SCC-7 cells and irradiation with 630nm LED light (power density 30mW/cm2, green=DCFH, blue=nucleus); F) Quantitative flow cytometry analysis of the fluorescence of TB after SCC-7 cells incubated with TB-B (10 μM) and 2TB-B@CB[8] (5 μM) followed by irradiation with 630nm LED light (black line=control, red line=TB-B, green line=2TB-B@CB[8], inset: mean fluorescence intensity (MFI) of DCFH).

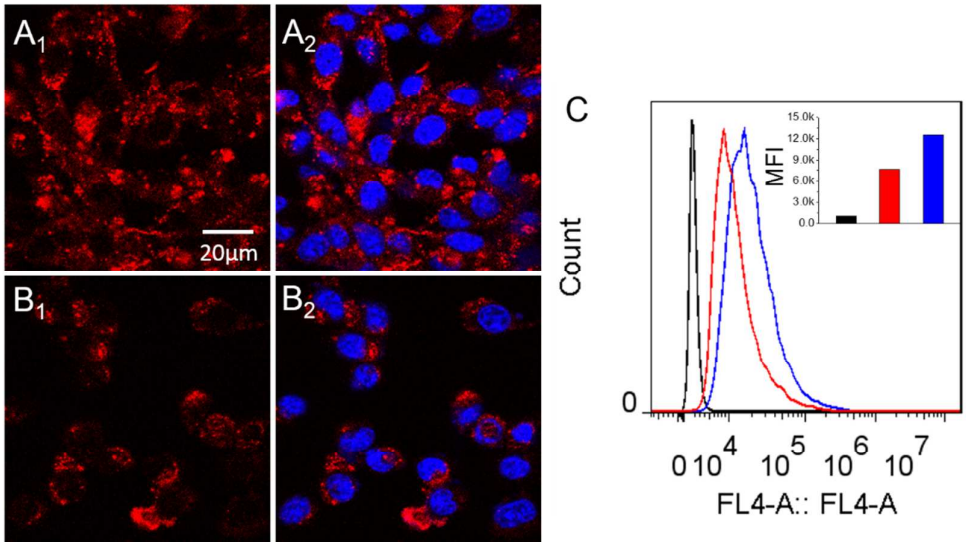

Figure S11 A-B) Confocal microscopy images showing SCC-7 cells incubated with A) 2TB-B@CB[8] (5 μM) and B) 2TB@CB[8] (5 μM) (red=TB, blue=nucleus); C) Quantitative flow cytometry analysis of the fluorescence of TB after SCC-7 cells incubated with 2TB-B@CB[8] (5 μM) and 2TB@CB[8] (5 μM) (black line=control, red line=2TB@CB[8], green line=2TB-B@CB[8], inset: mean fluorescence intensity (MFI) of TB).

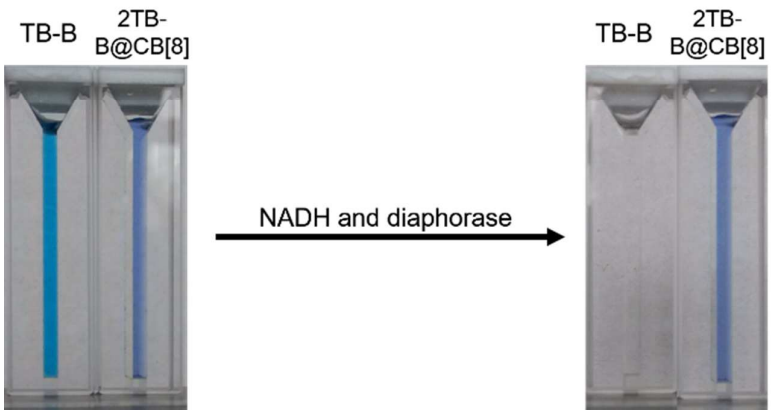

Figure S12. Color changes of TB-B (20 μM) and 2TB-B@CB[8] (10 μM) before and 30 min after the appearance of NADH (0.45μmol) and diaphorase (0.05mg).

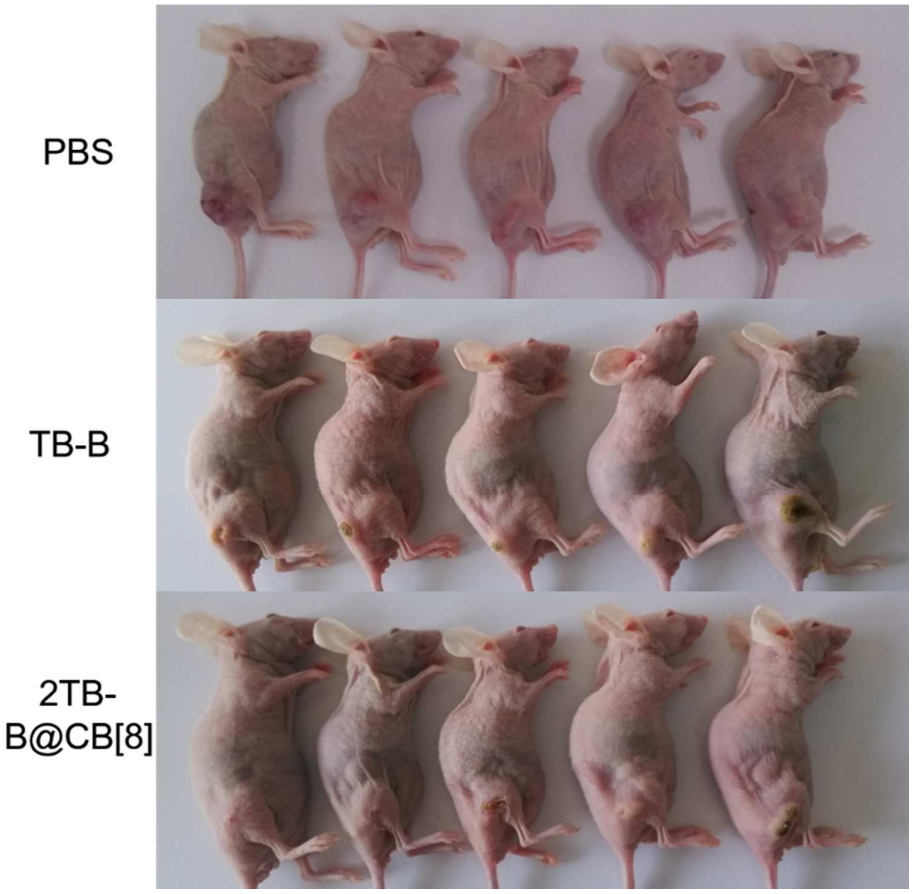

Figure S13. Images of the mice at the 12th day after treatment.

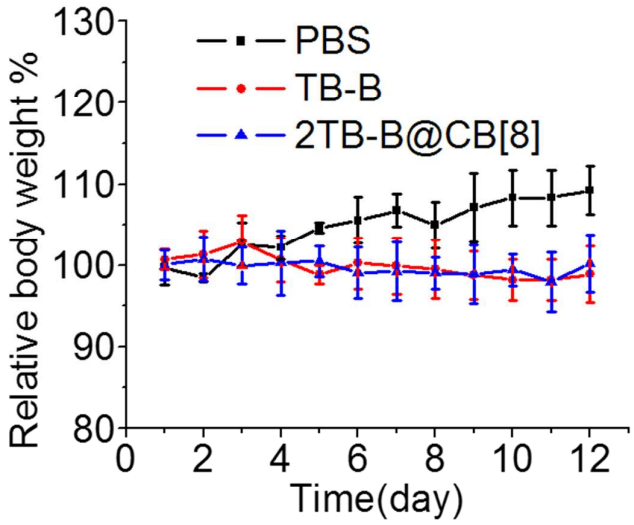

Figure S14. Relative body weight change during the treatment.